Engineering and Technology Journal e-ISSN: 2456-3358
Volume 09 Issue 02 February-2024, Page No.-3530-3537
DOI: 10.47191/etj/v9i02.14, I.F. – 8.227

Design and Implementation of Sensored Brushless DC Motor Control Using dsPIC30F4012 for CW/CCW Bidirectional Rotation

Yusie Rizal[1], Sarifudin[2]
[1,2] Department of Electrical Engineering, Politeknik Negeri Banjarmasin, Banjarmasin, Indonesia

ABSTRACT: This paper presents the development of BLDC (Brushless DC) motor control based on dsPIC30F4012. The system is designed to control motor rotation in clockwise (CW) and counter clockwise (CCW) directions. There are 3 input pins used to facilitate the control interface, namely ground (GND) pin, control (CTRL) pin and enable (EN) pin. An analog input was assigned as command input for rotation in CW/CCW direction. The CTRL pin input has full-scale of analog input that comprises of three regions, namely CCW rotation input (0V~2.4V), CW rotation input (2.6V~5V), and neutral input (2.5±0.1)V as the deadband. The commutation sequences of six steps for direction of motor rotation, while P-I (Proportional-Integral) controller is used to control the motor current. The control law and commutation sequences are implemented in single chip dsPIC30F4012 microcontroller. To verify the system performance, we test the system implementation to drive BLDC motor and measured current are sent to the host PC through serial communication. From the experimental results it is shown that the realizing P-I controller is good performance in small frequency where the bldc motor current can follow the input commands. The bandwidth of motor control to characterize the performance of designed system is also presented.

KEYWORDS: BLDC motor, motor driver, PI controller, dsPIC30F4012 microcontroller.

I. INTRODUCTION

Brushless DC (BLDC) motor have used in many mechatronics application from robotics, appliances, medical, vehicles to aerospace. In mechatronics and robotic systems, brushless dc (BLDC) motors have been used as replacement for conventional brushed dc motors because of high effeciency, high dynamic response, long operating life, low maintenance and noiseless operation for higher speed range [1]. One of the control problems in BLDC motor and can be considered as fundamental problem is to regulate motor current. For example, in multiple-loop control for speed control, the current loop control exist as inner-loop in control structures [2],[3]. The other control problems are speed control and position control. This paper discussess the development of current control for sensored brushless dc motor for bidirectional rotation using P-I controller.

Numerous studies have discussed the current controls in three phase BLDC motor. Different approaches both in current measurement strategies and current control methods have applied to BLDC motors [3],[4],[5],[6],[7]. Dixon, et al. [4],[5] proposed current controlled modulation technique based on generation of quasisquare-wave current in which two shunt resistors (instead of one) are used to sense two phase currents and then rectified it to obtain DC (voltage) signal. Chu, et al. [3] used one shunt resistor to sense the current as feedback to compare with desired reference current, and then PI control is implemented for over-current protection. Kos, et al. [6] realized the current measurement for current control using single current transducer, and then two control methods, that is, PI regulator and discontinuous sliding mode regulator are compared by spectral analysis. Azam, at al. [7] proposed new current blocking strategy by modifiying the original current control structure of hysteresis control to block motor current from batteries in order to avoid a waste of energy due to the current drawn in vehicle applications. The current control of BLDC motor using PI control is still widely used because of its simplicity and easy to apply [4],[5],[3],[6]. However, current hysteresis control is considered as the simplest closed-loop control scheme [7]. In this paper, we consider the current control based on PI to control the direction of BLDC motor. The given command is the analog signal with a range from 0~5V. This signal is then converted through analog-to-digital conversion by microcontroller and use this command to control motor direction. In the system design, two shunt resistors are used to measure current phase of BLDC motor when the corresponding motor phase is excited [4],[5]. The measurement of the current phase is then compared with the input command.

This paper presents the design and implementation of brushless dc motor (BLDCM) control for both clockwise (CW) and counter clockwise (CCW) rotation. In this system, a full-scale of analog input (0V~5V) is divided into two regions of input current: a negative input commands (0V~2.4V) and positive input commands (2.6V~5V) which correspond to CCW and CW rotation, respectively. In this paper, the current control based on Proportional-Integral (P-I) control algorithm and BLDCM commutation sequences are discussed. The commutation sequences from three hall sensors input are used to manage the rotation of BLDCM, while P-I controller is used as a current phase motor control. Moreover, the overall system was implemented in dsPIC30F4012 from Microchip and the controller law was written in C. To verify the performance of the system, the current phase and input command data were sent to host PC via serial communication (UART) RS232 with 19200 baud rates. For the host PC side, an interface program was developed using Borland C++ Builder 6 via ComPort Library. The result shows that the realizing controller has good performance where the BLDCM with no load can follow input commands in different operating ranges (±100mA, ±200mA and ±300mA).

II. BRUSHLESS DC MOTOR

A. System Model

In this section, we discuss the simplified mathematical model of BLDC motor, the electrical commutation control for forward-reverse operation, and current measurement strategy. We consider the BLDC motor of BLDC56 from TECO Electro Device (model DBT566S32A) in which the hall effect sensor switch and motor windings are shown in Fig. 1. The sensored bldc motor has three hall sensors to detect the position of the rotor. The sensor outputs may have high or low logic levels which correspond to '1' and '0' logic numbers, respectively. The combination of high and low logic state of the three sensors give six possible states and based on which state the rotor has, then the switching MOSFET are triggers to drive the motor.

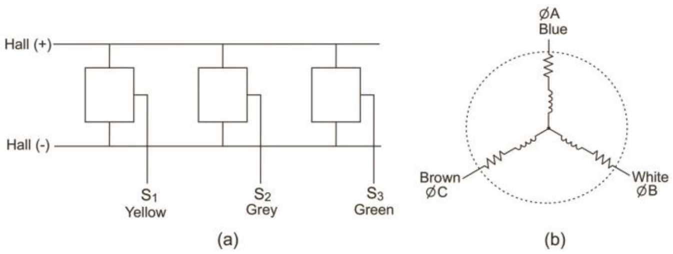

Fig. 1. Schematic diagram of BLDC motor: (a) Hall effect sensor, and (b) Three phase BLDC Motor.

The simplified model of BLDC motor [8] can be represented as given in Eq. (1).

$$\begin{bmatrix} u_a \\ u_b \\ u_c \end{bmatrix} = \begin{bmatrix} R & 0 & 0 \\ 0 & R & 0 \\ 0 & 0 & R \end{bmatrix} \begin{bmatrix} i_a \\ i_b \\ i_c \end{bmatrix} + \begin{bmatrix} L-M & 0 & 0 \\ 0 & L-M & 0 \\ 0 & 0 & L-M \end{bmatrix} \times \frac{d}{dt} \begin{bmatrix} i_a \\ i_b \\ i_c \end{bmatrix} + \begin{bmatrix} e_a \\ e_b \\ e_c \end{bmatrix} \quad (1)$$

where *R*, *L*, and *M* are phase resistance, self-inductance of all phases and mutual inductance between phases, respectively. i_a, i_b, and i_c are phase currents; e_a, e_b, and e_c are trapezoidal back-EMF, and u_a, u_b, and u_c are phase voltages. The system in (1) is standard model for BLDC motor. Let suppose that PWM signal *u* is generated by controller unit, one may use simplified model given in [9] as follow

$$v = R_m i + k_E \omega_r \quad (2)$$

where

$k_E = \frac{2}{3}(k_e + k_e + k_e), v(t) = v_{pwm} - v_0 sign(u), R_m = \frac{2}{3}(R + R + R)$ and $R = R_a = R_b = R_c$. Note that v_{pwm} is mean-value of the pulse-width modulated voltage, v_0 is voltage drop, and k_e is back-EMF constant. The equation of motion is given [8] by

$$T_e = J\frac{d\omega_r}{dt} + B\omega_r + T_l$$

J, B, T_e, T_l, and ω_r are moment inertia, viscous friction, electromagnetic torque, load torque and rotor angular velocity, respectively.

$$T_e = k_T i \quad (3)$$

in which k_T is the torque constant. The system parameter of system is given in Table I.

Table I. BLDC56 Specification (TECO Electro Device Co).

Parameter	Symbol	Value	Units
Rated Voltage	V	24	V
No Load Speed	S_{NL}	4400	rpm
Continuous Torque	T_C	1.93	kgf-cm
Continuous Speed	S_C	2700	rpm
Continuous Current	I_C	3.75	A
Continuous (output) Power	P_{OUT}	50	W
Number of Poles	-	8	-
Resistance	R	1.3	Ω
Winding Inductance	L	1.8	mH
Weight	W	0.6	kg
Peak Torque	T_P	5.7	kgf-cm
Peak Current	I_P	10	A

B. Electrical Commutation for Sensored BLDC motor

BLDC motors do not have brushes or commutation mechanism, instead, their rotors are electronically commutated and thus significantly improve mechanical reliability. In three-phase BLDC motor with 120° conduction, the commutation occurs at every 60° of electrical angles. Three Hall sensors (S_1, S_2, S_3) are used to detect rotor position where the sensors are separated in 120° to each others. The voltage of Hall effect sensors are produced when the magnet on the rotor moves near the sensor, the voltage signal is simply represented by '1' or '0' code. To rotate the motor in forward/reverse direction, one needs to know the codes of Hall effect sensors which is corresponds to the firing mosfets. Table IIa and IIb show the corresponding Hall effect sensors and mosfets for driving motor in CW and CCW, respectively.

Table IIa. Electrical Commutation for CW rotation [10]

Sensor Output			Driver Output			Status
S_1	S_2	S_3	ØA	ØB	ØC	Phase
0	0	1	-	HI	LO	4
0	1	1	HI	-	LO	3
0	1	0	HI	LO	-	2
1	1	0	-	LO	HI	1
1	0	0	LO	-	HI	6
1	0	1	LO	HI	-	5

Table IIb. Electrical Commutation for CCW rotation [10]

Sensor Output			Driver Output			Status
S_1	S_2	S_3	ØA	ØB	ØC	Phase
0	0	1	-	LO	HI	\4
0	1	1	LO	-	HI	\3
0	1	0	LO	HI	-	\2
1	1	0	-	HI	LO	\1
1	0	0	HI	-	LO	\6
1	0	1	HI	LO	-	\5

In Fig. 2, (G_1,G_2), (G_3,G_4), and (G_5,G_6) are the higher and lower mosfets that correspond to phase A, phase B, and phase C, respectively. For example, that the motor is rotating and the code of Hall effect sensors is given by (S_1, S_2, S_3,)=(0,1,0) (third row in Table IIa). Then, to rotate BLDC motor in forward (CW) direction, the mosfets (G_1,G_4) must be turned ON while (G_2,G_3,G_5,G_6) must be turned OFF. Likewise, if at that point the motor is required to rotate in reverse (CCW) direction, then according to Table IIa, (G_2,G_3) are turned ON while the rest turn OFF.

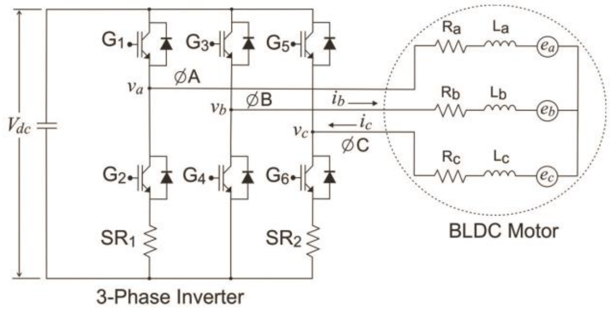

Fig. 2.Equivalent circuit of BLDC motor drive

By using look up table that given in Table IIa, the motor's rotation can be controlled for forward/reverse direction. However, in the real applications, when the motor is rotating in one direction especially in high speed, it is not possible to change its direction suddently due to phase current and motor inertia. In fact, this task must be avoided and in this paper, the use of PI controller and motor commutation controller are discussed in order to change motor direction smoothly.

III. RESEARCH METHOD

A. Inverter and Current Sensing

The BLDC motor that used in this system is the motor model of DBT566S32A from TECO Electro Device Co. where the parameters of the system is given in Table III. In Fig. 2, six mosfets are used to perform pulsewidth modulation (PWM) inverter of voltage-source configuration with constant dc-link voltage in which wye-connected three-phase square-wave BLDC motor is driven. The rotor position which determines the switching sequence of the mosfet transistors is derived from Hall sensors as given in Table IIa and IIb.

Two shunt resistors are used to measure the current phase, however, only one current control-loop active at any time [11]. They are located between lower mosfet and ground as shown in Fig. 2. It might be possible to use only a single shunt resistor instead of two as discribed in [12],[13]. These shunt resistors are mounted to INA225 as a current-sense amplifier with voltage-output and programmable-gain. The shunt-resistor of PWR221T-30 is used with specification of 20 mΩ, 5%, and 30W for resistance, resistor accuracy, and power dissipation, respectively.

From the specification of BLDC motor in Table I, the rate of continuous current is 3.75 A, and thus, the maximum output-voltage is 3.75 A x 20 mΩ = 75 mV. By choosing the programmable-gain of INA225 to set as 50 V/V, then the maximum output-voltage is 75 mV x 50V/V = 3.75 V (which is less than the allowable maximum limit voltage input 5 V of I/O Analog-to-Digital conversion in dsPIC30F4012). However, there are other optional programmable-gain values, namely, 25 V/V, 100 V/V, and 200 V/V. From the similar calculation mentioned above, it is found that gain value of 100V/V would exceed the maximum allowable analog input of 5 V in dsPIC30F4012, while choosing 25 V/V would only give too small voltage-output, that is 1.875 V for maximum current of 3.75 A.

The input command is given by external analog voltage to analog input in dsPIC30F4012. The maximum input for analog input A/D port is 5 V. Thus, to facilitate two even input current commands (forward and backward rotations), the analog input on dsPIC30F4012 side must be devided by two. This can be illustrated in Fig. 3(a) where the analog signal with 5V ranges is divided into 2.5V upper and 2.5V lower of operating commands for CW and CCW directions, respectively. These values must be calibrated such that the input command (I_{cmd}) has two operating regions with *c* is the STOP mode at the center point as shown in Fig. 3(b). It follows from the figure that the 0V is the maximum input command for CCW direction and 5V is the maximum input command for CW direction, while the center point (*c*) is the motor stop. To prevent the CCW or CW rotations, we define small dead-band such that the motor is perfectly stop around those band as shown in Fig. 3(b).

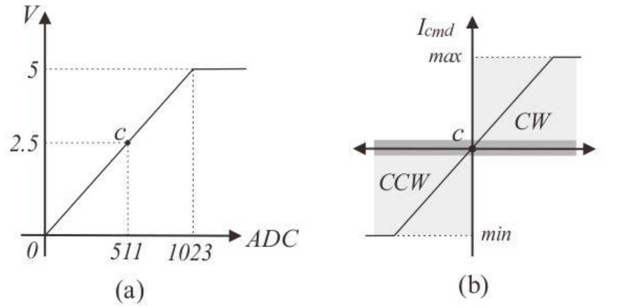

Fig. 3. Analog input: (a) input voltage, (b) input command

B. *Control Motor Based on PWM*

In this system where dsPIC30F4012 is used, the control output is facilitated by 3 PWM modules in which each module is responsible for controlling a pair of high and low mosfets. There are 6 PWM I/O pins with 3 duty cycle generators. Unlike a hysteresis current control, a PWM control does not have an inherent current control capability [14]. In implementation, we use PWM override control to manually drive the PWM I/O pins to specified logic states. This mean, based on Fig. 2 and Table I and II, we can define a six sequences of specified logic states for 6 PWM I/O pins to perform electrical commutation for the motor. Soft chopping method is used on lower mosfet in which (G_2-G_4-G_6) are always ON during the switching-on sequences, while the upper mosfet (G_1-G_3-G_5) are ON/OFF (based on PWM duty cycle) to produce less torque ripples [7]. We combine PWM generator and ON/OFF output for soft chopping. The lower mosfets are leaved On or without any duty cycles. Three High/Low PWM modules can be arranged to be in pair. It has 5 timers, input capture, analog-to-digital conversion, and 6 channel PWM. The period is given by

$$T_{PWM} = \frac{T_{CY} \cdot (PTPER+1)}{(PTMR\_PRESCALE)} \tag{4}$$

where T_{CY} is time cycle i.e, $1/T_{CY}$ = 4/(oscillatory frequency times PLLx), *PTMR_PRESCALE* is PWM time base register prescaler, and *PTPER* is PWM time base period register.

C. *Control Strategy*

1. *Input Command*

We consider the current control problem to control the direction of the motor based on PI controller. Fig. 3 show the input voltage range (left) and modified control input (right). Near 2.5 V there is deadband for stopping motor. The zero input and maximum input command are 0 V and 5 V, respectively, i.e. correspond to maximum input command in CCW operation and maximum input command in CW operation, resepectively. Since dsPIC30F4012 has 10-bits A/D, then following calibration is used

$$Y = X - c \tag{5}$$

Y is the nominal input command, *X* is the measured input command, and *c* is a center-point of constant, *c* = 1023/2. The value of *Y* can be negative/positive. However, the current phase of the motor is always positive. Hence, the sign (±) is used to determine the required direction of the motor (in CCW or CW direction).

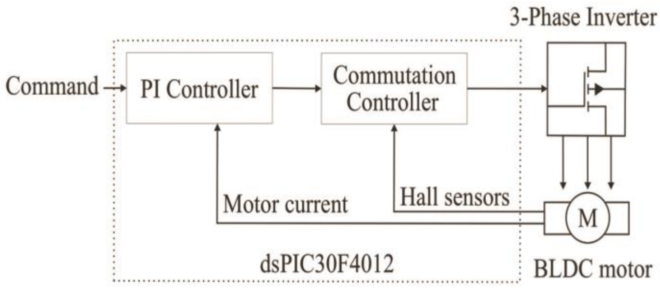

Fig. 4. Schematic diagram of Current Loop PI Controller

2. *Current Control Based on PI Controller*

The schematic diagram of current loop PI controller is as given in Fig. 4 where the controller is implemented in dsPIC30F4012 microcontroller. The PI controller and electrical commutation is implemented in single chip only. The command is analog input with 0~5V and the feedback from motor are hall sensors and current sense. The microcontroller is programmed using C language using C30 compiler from Microchip. The ICD3 In-circuit debugger/programmer is used to implemented by uploading the machine codes to microcontroller. The PI controller law is given as follow [4],

$$PI(t) = K_p e(t) + K_i \int_0^{t_1} e(t)dt \tag{6}$$

where *e(t)* is the current error at time *t* while K_p and K_i are the proportional gain and integration gain, respectively. The error *e* is given by

$$e = i^* - i \tag{7}$$

where i^* and *i* are the desired and actual currents, respectively.

D. *Frequency Domain and Control Bandwidth*

To measure the bandwidth of the control performance, we generate a sinusoidal input command inside microcontroller. Then the input command and output control are measured and sent to flash memory of dsPIC30F4012. There are total 2 kilobyte flash memory that can be used for this system. The measurement was calculated every 10 ms and stored in flash memory. In this research, we implement PI controller as discussed in previous section. The diagram of control system can be depicted in Fig. 4. The are two feedback of the controller, one is from Hall effect sensors and the other one is from shunt resistor of current phase measurements.

For harmonic input in the form of $x(t) = A_x \sin \omega t$, the output for linear system will be in the form $y(t) = A_y \sin(\omega t - \psi)$. The phase angle ψ, and amplitude ratio $M = A_y / A_x$ is given by [15] is given by

$$M = \sqrt{\frac{1}{1+\tau^2\omega^2}} \tag{8}$$

and

$$\psi = -\tan^{-1}(\tau\omega) \tag{9}$$

where ω and τ are the frequency and time constant, respectively. It is noted that at $\omega = 1/\tau$ where the amplitude ratio is M = 0.707, M = -3 dB (20 log (M)), and $\phi = -45°$. This frequency is known as the break frequency.

The measured data (input commands and motor currents) are the signals in time domain. These signals can be converted to frequency domain by using Fast Fourier Transform (FFT). The FFT algorithm can be written as follows

$$X(k) = \sum_{j=1}^{N} x(j)\omega_N^{(j-1)(k-1)} \tag{10}$$

where $\omega_N = e^{(-2\pi j)/N}$ is an N^{th} root of unity. The bode plot of the system is using the following equation

$$|Magnitude|(dB) = 20 \times \log_{10}\left(\frac{Y}{X}\right) \tag{11}$$

with X and Y are the magnitudes of input-output, respectively, where they are given by calculating using equation (10). The controller frequency bandwidth is determined when the system has BW = –3dB. dsPIC30F4012 has 2 kilobytes memory SRAM (2048 bytes), then we use this memory as a buffer to store the input command from IN1 and data of the current as the feedback. Since 2 kilobyte is not enough to store amount of measured data, then we send those data to PC through serial UART communication where we assigned the controller to send data every 500 ms. The measured data ADC (from input command and current phase is in a range of 500 μs).

E. Current Sensing and Data Acquisition

The current control with current feedback is used by following formulation:

$$Max\_val_{ADC} = Max\_volt_{ADC} \tag{12}$$

where Max_val_{ADC} = 1023 and Max_volt_{ADC} = 5V with the resolution of ADC is 5V/1024 = 0.00483V. We choose gain of current amplifier as 50 and 0.02 Ω with 5% tolerance for Shunt Resistance (R_{shunt}). If the current limit for the driver is set to (I_{shunt}) 3A, then the maximum of ADC value that allowed is

$$Voltage_{MAX} = I_{shunt} \times G \times R_{shunt} = 3V \tag{13}$$

The equivalent ADC value for the maximum current allowed in in (13) is

$$Value_{MAX} = \frac{3V}{5V} \times 1023 = 613.8 \approx 614. \tag{14}$$

This means for every 1 mV detected voltage across shunt resistor is equal to 1 mA (since the relation factor of R_{shunt} and gain is unity (0.02Ω x 50 V/V=1 ΩV/V). It is important to note that the maximum current command is 100 mA, because the motor has no load (as defined in system specification).

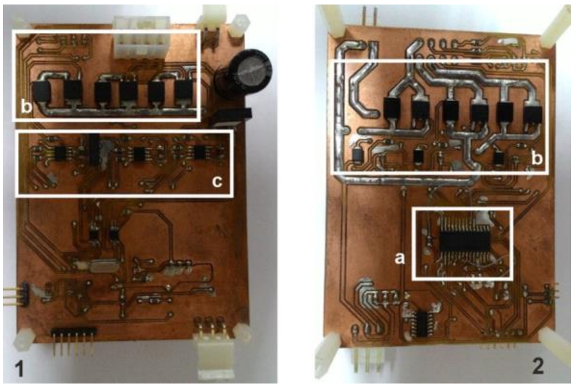

Fig. 5. Prototype of BLDC motor control: (a) Microcontroller dsPIC30F4012, (b) Mosfets and Schottky diodes, (c) Mosfet gate drivers

F. Experimental Setup

In this work, a motor controller board is design and developed based on dsPIC30F4012 microcontroller as given in Fig. 5. Two input commands of which labeled as 'ENABLE' and 'CMD' are provided to control the motor i.e to enable the motor and to control motor current using digital and analog inputs, respectively. The schematic diagram of system control of BLDC motor is shown in Fig. 6. The commutation sequences from three hall sensors input are used to manage the rotation of BLDCM, while P-I controller is used as a current phase motor control. The overall system was implemented in dsPIC30F4012 from Microchip and the controller law was written in C.

The experimental study was conducted to evaluate the performance of the control systems. BLDC motor was operated under no load conditions and different input commands were given to observed the system performances in bidirectional operation. The tuning of control gains (proportional and integral) are based on experimental study. In this study, the control gains for K_p and K_i are 1.0 and 0.2, respectively.

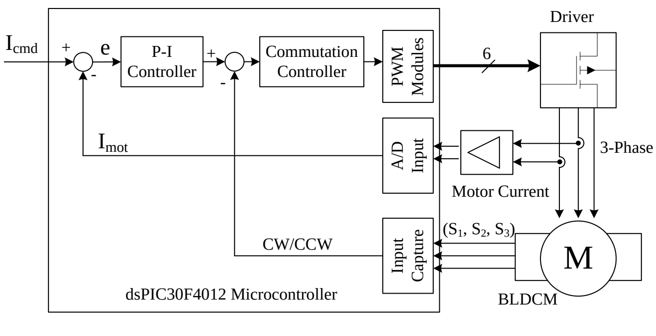

Fig. 6.Schematic diagram of BLDC motor control

To verify the performance of the system, the current phase and input command data were sent to host PC via serial communication (UART) RS232 with 19200 baud rates. For the host PC side, an interface program was developed using Borland C++ Builder 6 via ComPort Library of Djan Crenilla. This serial communication (UART) was interfaced to PC through COM1 with 19200 baudrate. The data captures in dsPIC30F4012 microcontroller sent through UART every 20 ms. Every 1 s the controller send these data to PC through serial RS-232 communication. The data that being stored are input command, output command, and current data. These three data are collected and saved in flash memory and then send to PC. The sinusoidal command that generated inside microcontroller were designed to have different frequencies, they are 1 Hz, 10 Hz, 100 Hz, 1 kHz. When the system is implemented, the input command and output signal can be captured to observe the performance of the system.

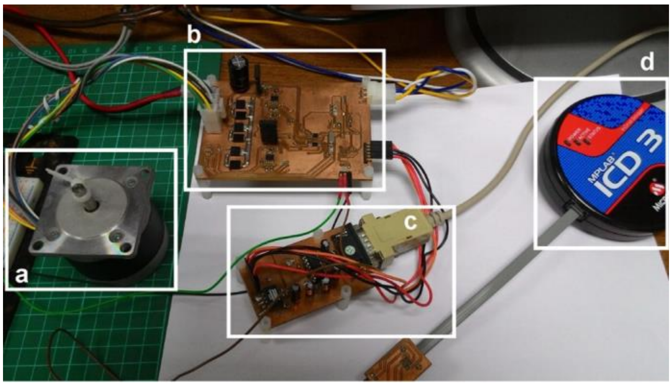

Fig. 7. Experimental Setup: (a) BLDC motor, (b) BLDC control board, (c) Serial communication board, (d) MPLAB ICD3 programmer

The designed control laws were implemented on dsPIC30F4012 (main controller) and the experimental setup is described in Fig. 7 and Fig. 8. In this Fig. 8, the function generator is used as input commands in which the sine functions with different frequencies were generated. Every 500 μs the main controller measures two phase currents and use this measurement as current feedback to updates its control law. Every 20 ms the controller send one series of data which consists of two data packages, the current command data and measured motor current. The data transmitted from microcontroller to the host PC are strings type with series of hexadecimal packages. The designated format package is consist of 11 bytes data, given as format:

$$[\%][d1][d2][d3][d4][\#][e1][e2][e3][e4][0x0d] \quad (15)$$

The received packages data are then processed in text buffers and plotted on X–Y coordinate axes. In Fig. 9, the user interface of serial communication between host PC and microcontroller dsPIC30F4012 is given.

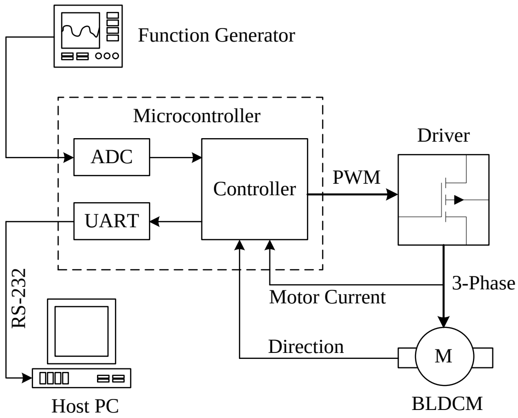

Fig. 8. Schematic diagram of experimental Setup

IV. EXPERIMENTAL RESULTS

The experiment is conducted to measure the performance of the controller system by using the experimental setup as given in Fig. 7 and Fig. 8. We provide the experiments with manual input with potentiometer as analog input, sinusoidal input, and different input commands to obtain the control bandwidth. These results are given in Fig. 10, 11, and 12, respectively.

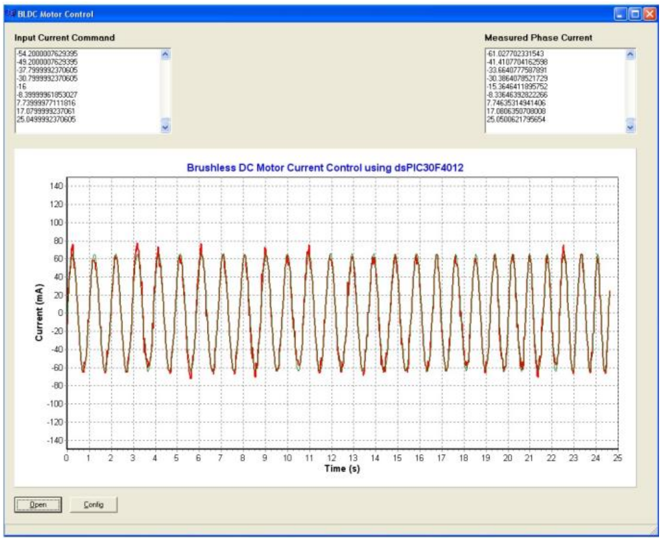

Fig. 9. User interface of serial communication to collect data from dsPIC30F4012

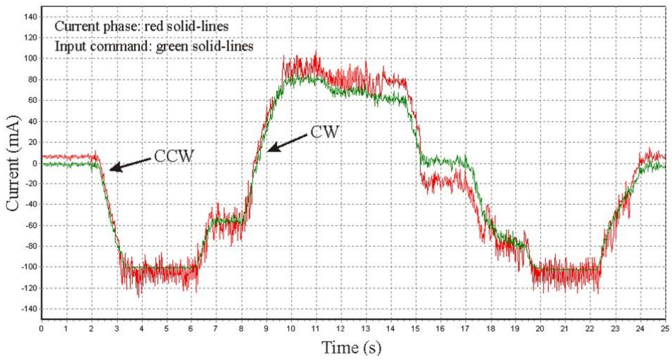

Fig. 10. Experimental result of current control with manual input command

In Fig. 10, it is shown the current motor obtained from manual input by changing the rotation of the potentiometer. This gives the analog input to I_{cmd} and after it converted to digital the controller follows the input command. In Fig. 10, the lower current input command (less than 0 mA) means the BLDC motor rotates in CCW, while the upper current input (above 0 mA) means the BLDC motor rotates in CW direction. The green solid-line represents the input command, and the red solid-line is system response. It is shown that the system response follows the input command. However, there are small discrepancy between input current command and measured phase current.

In Fig. 11, the input signal of sine wave generator with 1 Hz frequency, 3V peak-to-peak and 2.5V offset (this mean the signal swings from 1V to 4V) is given to the I_{cmd}. Fig. 11 shows the unit in Ampere and it is obtained from converting the analog voltage input to analog input command (in ADC). The blue solid line is the input command and the red line is the measured current response. It is shown that the current response of motor current can follow perfectly the input current command for given input frequency (of 1 Hz). When the frequency of sinusoid input signals is higher, the analog-to-digital conversion (ADC) have limited speed to convert the command, thus, it leads to system performance degradation.

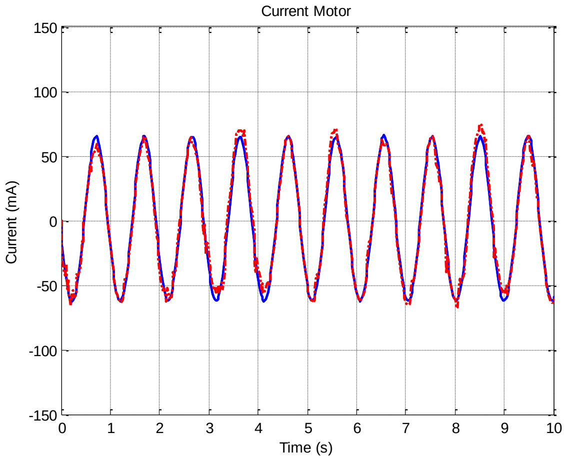

Fig. 11. Experimental result of current control with sinusoidal input command

From the Fig. 12, it is shown that the bandwidth of this system is approximately 3 Hz only. This means the system response is degraded when the frequency of sinusoidal input command is larger. The system response is too slow to follow the input command. From the experimental setup perspective, it is possibly that this system performance is due to the computation burden for a microcontroller dsPIC30F4012 to perform different tasks in a single chip, e.g. current control, electrical commutation, and serial communication. Thus, improvement for system performance can be done by separating the controller part and (serial) communication part. The measurement of system should be taken outside of the system, e.g. by measuring the input command and compare with the output speed. One way to solve this problem is by using separate microcontrollers e.g. using master-slave communication. Other possibility is by directly sending the measured data to another microcontroller and then, the second microcontroller performed the serial communication to host PC. However, different approach can also be applied by measuring the input command and current phase as well as motor speed using separate instrument measurements outside the controller.

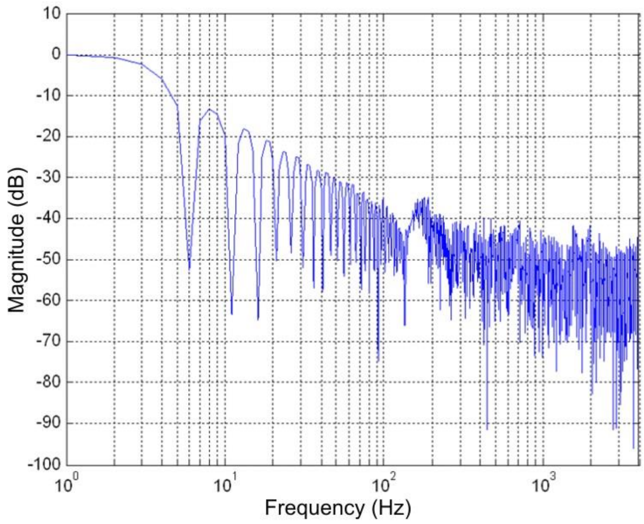

Fig. 12. Bandwidth of current control

V. CONCLUSION

In this paper the development of bldc motor controller based on dsPIC30F4012 to control the motor in CCW and CW directions. The P-I controller is employed to control current and motor rotation. We perform experimental works by manually giving input command and sinusoidal input command. From the experimental results it is shown that the system response can follow the input command perfectly if the frequency is smaller. This system performance can be shown in figure in bandwidth analysis. This drawback is possibly due to the computation burden where all tasks are performed in single chip. Some improvements can be taken by redesigning the overal system where dsPIC30F4012 microcontroller is employed to control the commutation and motor current only.

REFERENCES

1. W. Huazhang, "Design and Implementation of Brushless DC Motor Drive and Control System," *Procedia Eng.*, vol. 29, pp. 2219–2224, 2012, doi: 10.1016/j.proeng.2012.01.291.
2. J. C. Gamazo-Real, E. Vázquez-Sánchez, and J. Gómez-Gil, "Position and Speed Control of Brushless DC Motors Using Sensorless Techniques and Application Trends," *Sensors*, vol. 10, no. 7, pp. 6901–6947, Jul. 2010, doi: 10.3390/s100706901.
3. Jun-Uk Chu, In-Hyuk Moon, Gi-Won Choi, Jei-Cheong Ryu, and Mu-Seong Mun, "Design of BLDC

motor controller for electric power wheelchair," in *Proceedings of the IEEE International Conference on Mechatronics, 2004. ICM '04.*, 2024, pp. 92–97. doi: 10.1109/ICMECH.2004.1364418.

4. J. W. Dixon and L. A. Leal, "Current control strategy for brushless DC motors based on a common DC signal," *IEEE Trans. Power Electron.*, vol. 17, no. 2, pp. 232–240, Mar. 2002, doi: 10.1109/63.988834.
5. J. Dixon, M. Rodriguez, and R. Huerta, "Position estimator and simplified current control strategy for brushless-DC motors, using DSP technology," in *IEEE 2002 28th Annual Conference of the Industrial Electronics Society. IECON 02*, 2003, vol. 1, pp. 590–596. doi: 10.1109/IECON.2002.1187574.
6. D. Kos, M. Curkovic, and K. Jezernik, "FPGA Based BLDC Motor Current Control with Spectral Analysis," in *2006 12th International Power Electronics and Motion Control Conference*, Aug. 2006, pp. 1217–1222. doi: 10.1109/EPEPEMC.2006.4778568.
7. A. F. Noor Azam *et al.*, "Current control of BLDC drives for EV application," in *2013 IEEE 7th International Power Engineering and Optimization Conference (PEOCO)*, Jun. 2013, pp. 411–416. doi: 10.1109/PEOCO.2013.6564583.
8. R. Krishnan, *Permanent magnet synchronous and brushless DC motor drives*. CRC Press, Taylor & Francis Group, 2017.
9. Đ. Juričić, O. Moseler, and A. Rakar, "Model-based condition monitoring of an actuator system driven by a brushless DC motor," *Control Eng. Pract.*, vol. 9, no. 5, pp. 545–554, May 2001, doi: 10.1016/S0967-0661(01)00005-3.
10. W. Brown, "Brushless dc motor control made easy," 2002.
11. C. S. Berendsen, G. Champenois, and A. Bolopion, "Commutation strategies for brushless DC motors: influence on instant torque," *IEEE Trans. Power Electron.*, vol. 8, no. 2, pp. 231–236, Apr. 1993, doi: 10.1109/63.223976.
12. R. C. Becerra, T. M. Jahns, and M. Ehsani, "Four-quadrant sensorless brushless ECM drive," in *[Proceedings] APEC '91: Sixth Annual Applied Power Electronics Conference and Exhibition*, 1991, pp. 202–209. doi: 10.1109/APEC.1991.146165.
13. R. C. Becerra, M. Ehsani, and T. J. E. Miller, "Commutation of SR motors," *IEEE Trans. Power Electron.*, vol. 8, no. 3, pp. 257–263, Jul. 1993, doi: 10.1109/63.233281.
14. A. R. Paul and M. George, "Brushless DC motor control using digital PWM techniques," in *2011 International Conference on Signal Processing, Communication, Computing and Networking Technologies*, Jul. 2011, pp. 733–738. doi: 10.1109/ICSCCN.2011.6024647.
15. R. Firoozian, *Servo Motors and Industrial Control Theory*. Cham: Springer International Publishing, 2014. doi: 10.1007/978-3-319-07275-3.